engineering proceedings

MDPI

Proceeding Paper

Innovative Design and Prototyping of Reconfigurable Run-Flat Tire †

Gabriel Testa [1], Luca Esposito [2], Andrea Ceccacci [1,*], Gianluca Iannitti [1] and Nicola Bonora [1]

[1] Department of Civil and Mechanical Engineering, University of Cassino and Southern Lazio, IT-03043 Cassino, FR, Italy; gabriel.testa@unicas.it (G.T.); gianluca.iannitti@unicas.it (G.I.); nicola.bonora@unicas.it (N.B.)
[2] Department of Industrial Engineering, University of Naples Federico II, IT-80138 Napoli, NA, Italy; luca.esposito2@unina.it
* Correspondence: andrea.ceccacci@unicas.it
† Presented at the 53rd Conference of the Italian Scientific Society of Mechanical Engineering Design (AIAS 2024), Naples, Italy, 4–7 September 2024.

Abstract: Tire puncturing is one of the main causes of accidents and/or traffic interruptions, leading to unsafe and unsustainable mobility scenarios. Insert-supporting Run-Flat systems can be a strategic technology to improve tire performance, but further developments are needed to improve system reliability, modularity, and efficiency. A novel Run-Flat system was proposed in the present study to address specific features. The concept was developed by exploiting numerical simulation tools, enabling a comprehensive system assessment. In addition, a technological demonstrator was manufactured employing rapid prototyping techniques based on 3D printing processes.

Keywords: Run-Flat; tire; prototyping; 3D printing; numerical simulation

Academic Editors: Umberto Galietti, Gabriele Arcidiacono, Enrico Armentani, Davide Castagnetti, Vigilio Fontanari and Aurelio Somà

Published: 21 February 2025

Citation: Testa, G.; Esposito, L.; Ceccacci, A.; Iannitti, G.; Bonora, N. Innovative Design and Prototyping of Reconfigurable Run-Flat Tire. *Eng. Proc.* **2025**, *85*, 25. https://doi.org/10.3390/engproc2025085025

1. Introduction

Pneumatic tires are the most comprehensively used tires in various mobility applications; this extensive diffusion is mainly due to their advantages when compared with non-pneumatic tires: good trade-off between comfort and driving performances, easiness of rolling over obstacles, lightness, and low noise. This kind of device's drawback is primarily associated with the vulnerability to puncturing and associated consequences [1], leading to unsafe and unsustainable mobility scenarios [2]. In the past decades, several solutions have been proposed to overcome the eventuality of pressure loss in tires to mitigate the consequences of tire puncturing, enabling the pilot to maintain/preserve the control of the vehicle, allowing driving at limited speed, and ensuring the safety of the vehicle's occupants. Different categories of Run-Flat systems are employed, summarized as follows:

- Sidewall Insertion support;
- Wheel–ring support;
- Band-reinforced;
- Self-healing.

The sidewall insertion solution is one of the most diffused systems (Figure 1a), especially for road applications; it is also indicated as "self-supporting" since it consists of an additional layer in the side of the tire, able to withstand the vehicle's dynamic forces in case of partial or total pressure loss. In wheel–ring support, the ring fixed on the metallic rim does not take part in the interaction between road and vehicle in normal operating conditions; only in case the pressure is lost the support action of the tire is replaced by the

ring (Figure 1b). Band-reinforced tires consist of specifically built tires hosting an additional reinforcement layer, placed inside the tire crown, disposed in the hoop direction, and shaped as a helical coil [3,4], as represented in Figure 1c. In the self-healing solution, the inside of the tire has a thick, rubbery, and very sticky polymer that can seal the puncture, avoiding or reducing the pressure loss (Figure 1d).

Among the critical aspects of Run-Flat systems, overheating is one of the occurrences to be accounted for, as highlighted by several authors [5–7]. This phenomenon is strongly linked to the viscous behavior of elastomeric materials and their response to cyclic loading/unloading, showing energy dissipation due to heat production, leading to temperature increase. The knowledge of cyclic behavior of elastomeric materials is crucial to understand energy degradation and transformation inside the material; for this reason, this is one of the main topics investigated by several authors using advanced techniques [8]. In addition to viscous effects inside the material, a supplementary temperature increase is usually determined by friction between surfaces. Those phenomena worsen when heat dissipation is inhibited (e.g., inside the tire). The combination of unfavorable conditions can cause intense rising heat accumulation, leading to catastrophic failures due to the drastic reduction in mechanical properties of these rubber-like materials. Managing temperature inside the material is strongly linked to the duration of Run-Flat systems and their ability to travel for many kilometers after the puncturing occurrence. In the present study, the proposed novel Run-Flat system named Hero-Belt can potentially enhance some critical features of this kind of device.

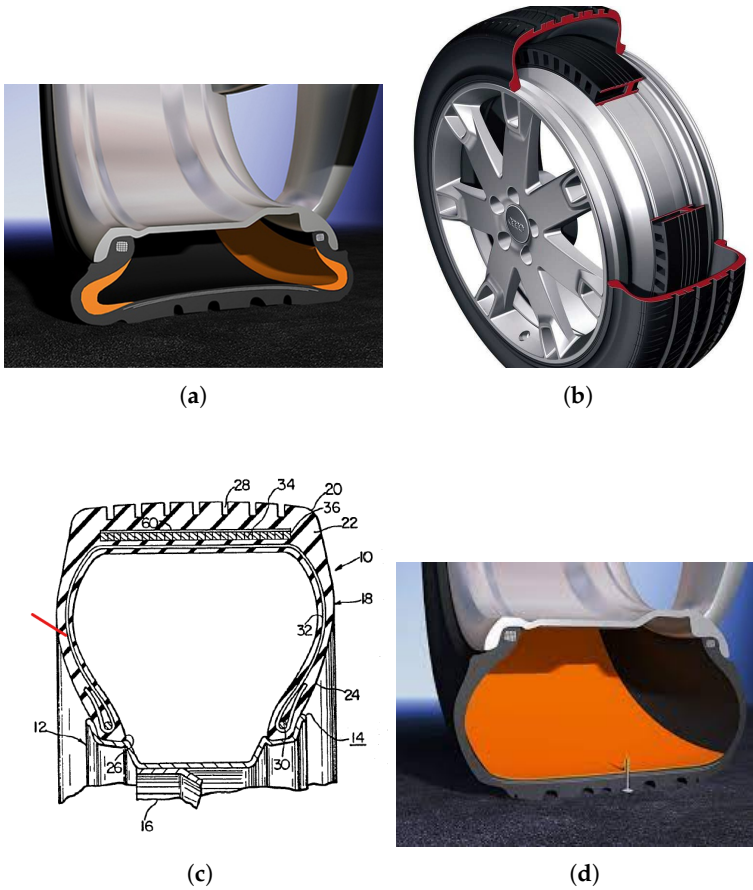

(**a**) (**b**)

(**c**) (**d**)

Figure 1. Different Run-Flat systems. (**a**) Sidewall insertion support [9]. (**b**) Wheel-ring support [10]. (**c**) Band-reinforced [3]. (**d**) Self-healing [11].

2. Concept Development

The reference application domain considered is a generic mid-weighted vehicle for heavy-duty uses in extreme operating conditions, like off-road tracks, extremely hot or cold environments, remote and hostile natural environments, and unavailability of spare tires. Those conditions could make it difficult to operate the tire replacement, making it necessary to keep on without any stop for relatively long distances. The reference wheel considered for the study case is a generic steel rim, enabling the use of a tire whose characteristics are reported in Table 1. Figure 2 reports the drawing of the wheel rim.

Table 1. Reference characteristics for the application.

Width [mm]	Rim Radius [inch]	Ratio Width/Height	Load Index	Allowable Max Weight [kg]
245	17.5	70	136	2240

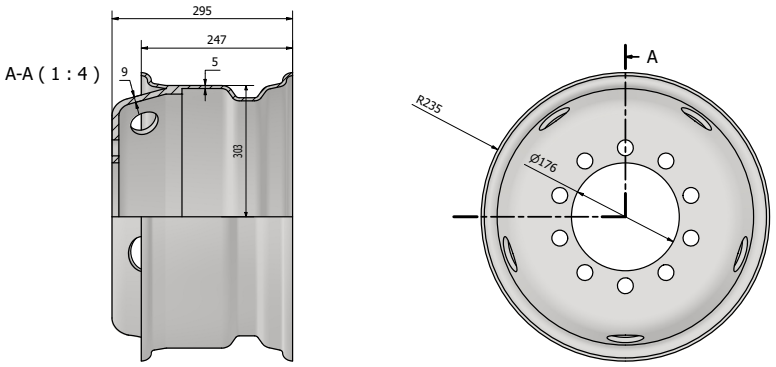

Figure 2. Representation of wheel rim.

The basis of the concept is for wheel-ring support to be fitted on the metallic rim; in this configuration, the system does not support the vehicle moving under normal operating conditions, and it only works in case of pressure loss. Differently from the standard Run-Flat wheel ring, the idea associated with HeroBelt is to have radially distributed knobs disjointed from each other rather than a unique ring made of continuous material. This feature may allow for a better distribution and dissipation of heat generated by deformation processes and friction in the rolling process. The gaps in the elastomeric material may inhibit heat-conductive flow between one knob and another. In this way, during the cyclic rolling phenomena, each knob would experience a rapid and brief temperature increase during the loading/unloading, followed by a longer unloaded angular phase, during which the knob can cool off, avoiding heat transfer to the contiguous knobs (Figure 3). Moreover a multi-component modular design could allow for the obtainment of a reconfigurable multi-platform system.

An additional aspect to be considered in the design process is the kinematic performance of the system. The gap between one knob and the other, associated with a block-shaped knob, would cause a higher rolling resistance, a discontinuous movement related to vibrations and dynamic forces. For this reason, the shape and distribution of the knobs has been carefully evaluated. To obtain a gradual loading/unloading phase, it was necessary that, in the contact area, the unloading of the knob, and the loading of the adjacent one, must be partially simultaneous. This kind of behavior was obtained by employing an arrow-shaped knob (or V-shaped). To ensure continuous rolling, the density of the knobs in the hoop direction plays an important role. The distribution of knobs was determined to ensure at least three simultaneously contacting knobs: considering a casual time frame, one could see a fully loaded knob, a front knob in loading, and a rear knob in unloading. That is the minimum condition required.

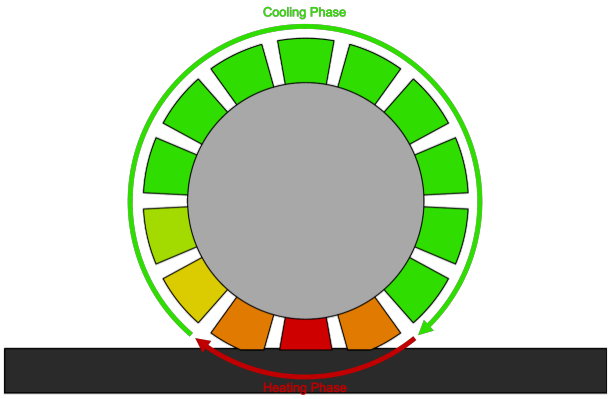

Figure 3. Representation of the thermal cycle expected.

2.1. Run-Flat System

The design activity produced a system composed of rubber-made knobs circumferentially distributed and connected by a metallic belt, entitled Hero-Belt. The belt system is designed to be fitted on the wheel rim; the pretension force imposed on the metallic chain is responsible for securing the array of knobs on the wheel. Representation of Hero-Belt system is reported in Figures 4 and 5. A total of 36 knobs proved to be a good trade-off in terms of structural resistance and contact surface with the road. Each knob has its own support (or chain-link); each chain link is connected to the previous and the next using bolted connections, enabling a rotational degree of freedom between chain link pairs.

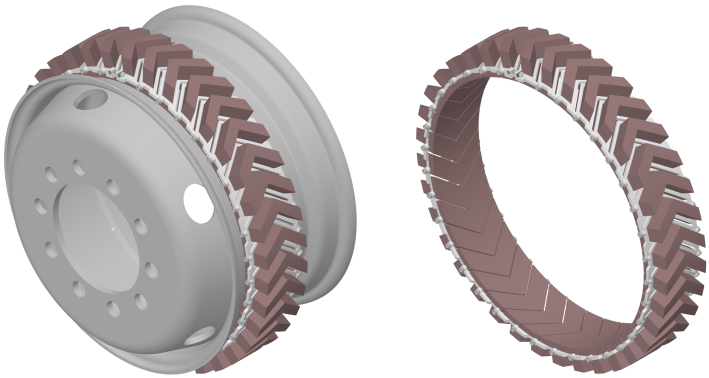

Figure 4. 3D CAD model of Hero-Belt system: including wheel rim (**left**), without wheel rim visibility (**right**).

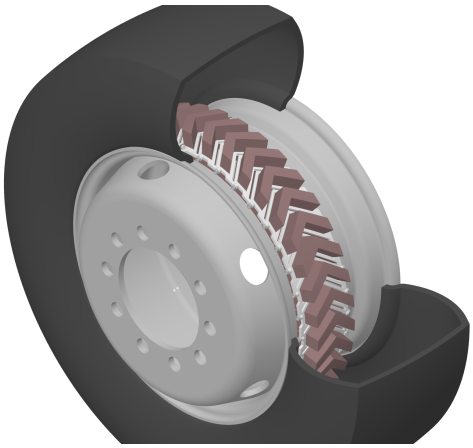

Figure 5. 3D CAD model of Hero-Belt system, including tire visibility in partial section.

2.2. Knob Development

Knobs are designed to form an arrow shape (or V-shape) to ensure continuous motion and a smooth transition from consecutive contacting knobs. The definition of the geometrical feature of the knobs was derived from different aspects considered: structural resistance of the items, compliance with geometric constraints, kinematic performances and motion continuity, feasibility of manufacturing aspects, and feasibility of assembly and disassembly operations. Several design loops have been necessary to determine a feasible geometry; different models have been formulated and evaluated iteratively; the overall geometry of the preliminary design is reported in Figures 6 and 7.

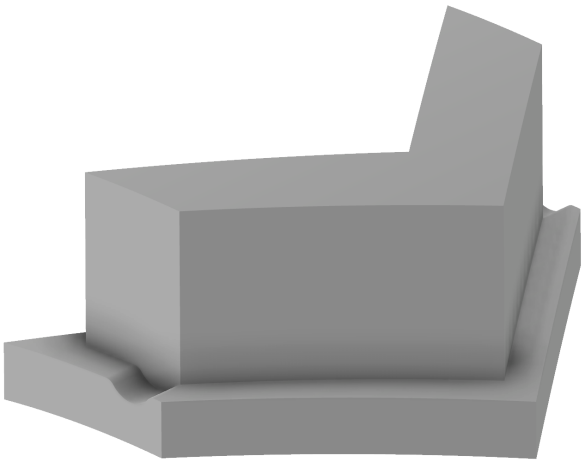

Figure 6. Knob isometric view.

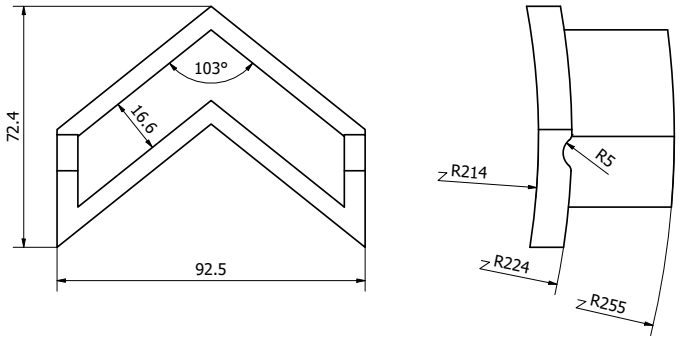

Figure 7. Knob top and lateral views. Overall dimensions reported.

The material for the knobs was chosen considering desired mechanical characteristics and the availability of literature data needed for the structural modeling. Filled rubber class material was set for the knobs: a material similar to the ones used for tire manufacturing since the component is responsible for the interaction between the wheel and the road. The open literature was reviewed to evaluate and select suitable models and associated parameter sets. Different material models have been proposed to describe the complex mechanical behavior of elastomeric materials. Such materials show a non-linear relationship between stress and strain from the elastic deformation state. Figure 8 shows a typical hyperelastic behavior associated with a rubber-like material subjected to tensile loading.

Mooney–Rivlin, Yeoh, Ogden, and Arruda–Boyce are the main material models used to describe elastomers' behavior. Several authors compared different models, assessing their ability to describe experimental data and the easiness of determining effective parameter sets associated with the model. Phromjan et al. [12] performed compressive tests on filled rubber compounds; material models were compared by implementation in finite

element simulations to find agreement between numerical and experimental results. The comparison highlighted that the Ogden model provided the best results. A full-scale test was conducted on truck tires in loading condition; numerical simulations of the test, using selected models, provided a good prediction of the reaction force exerted by the tire. Jebur et al. [13] performed a tensile test campaign on filled rubber specimens and reproduced the experimental test using finite element analyses: different material models were implemented to evaluate their suitability. The authors found the best results when comparing numerical and experimental results, using the Ogden model to describe material in numerical simulations. Beyond the two previously cited works, the Ogden model is recognized as a good trade-off between effectiveness and complexity and it has been employed to describe the material of knobs.

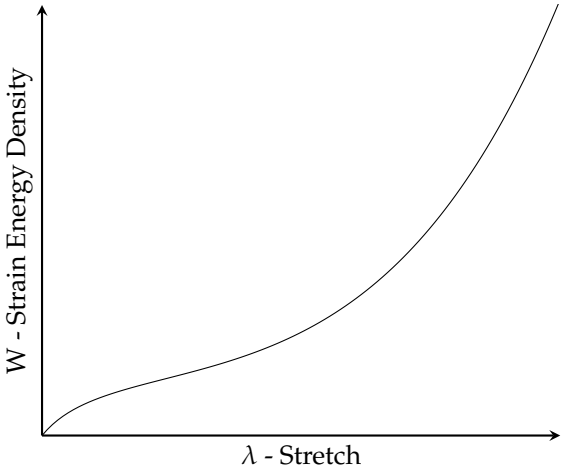

Figure 8. A typical stress–strain curve for elastomeric materials.

The Ogden model, proposed by R.W. Ogden in 1972 [14], is based on the expression of the constitutive model using a strain energy function, defined as a linear combination of the principal stretches: λ_1, λ_2, λ_3 (Figure 9).

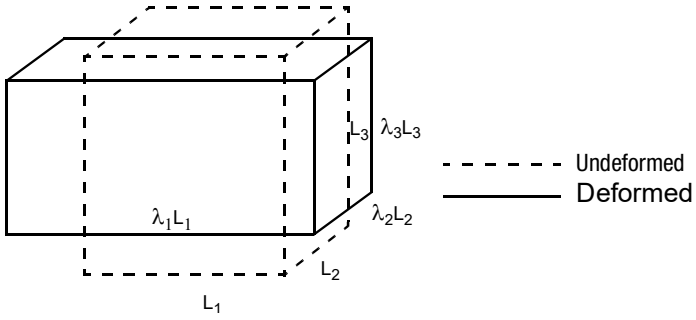

Figure 9. Material elementary volume in an undeformed and deformed state; indication of principal stretches.

The strain energy function is expressed as a linear combination of the invariants $\Phi(\alpha)$; defined as in (1).

$$\Phi(\alpha) = \frac{\lambda_1^{\alpha} + \lambda_2^{\alpha} + \lambda_3^{\alpha}}{\alpha} \quad (1)$$

Indicating with W the strain energy function proposed by Ogden, the expression has the form reported in (3).

$$W = \sum_{k=1}^{N} \mu_k \cdot \Phi(\alpha_k) \quad (2)$$

$$W = \sum_{k=1}^{N} \frac{\mu_k}{\alpha_k} \cdot (\lambda_1^{\alpha_k} + \lambda_2^{\alpha_k} + \lambda_3^{\alpha_k} - 3) \quad (3)$$

where μ_k and α_k are material constants, and N is the number of terms, of which the latter usually varies from 1 to 3.

Several authors approached the study of filled rubber for automotive application to provide Ogden parameter-sets, for computational purposes [14–16]. Different results have been found in terms of strain energy density with respect to stretch and associated parameters. Wide scatter of mechanical properties is commonly recognized as an inherent characteristic of this material class by manufacturers and researchers. Differences in the mechanical response can be mostly attributed to different filler content, rubber chemical composition, and thermal processes applied during manufacturing. To develop a preliminary design for the knob, the requirement for material characteristics was set as an intermediate option in terms of stiffness; for this reason, in the following sections, the reference material for the knob will be the one from Fu et al. [17], the parameters of which are reported in Table 2.

Table 2. Material parameters, by Ref. [17].

α_1	μ_1	α_2	μ_2	α_3	μ_3
3.666	4.688	3.870	−4.055	−13.598	−0.03249

3. System Analysis

A numerical simulation of the Hero-Belt system was performed to obtain a comprehensive assessment of the system. The analysis investigated the interaction between the system and the ground, replicating the rolling phenomena. The simulation involved the modeling of the different parts of the system: knobs and chain links assembled on the wheel rim, rolling on flat ground (Figure 10). A full 3D transient analysis was set up using the tool Ls-Dyna; bodies involved in the analysis are specified in Table 3, including modeling information associated with each body.

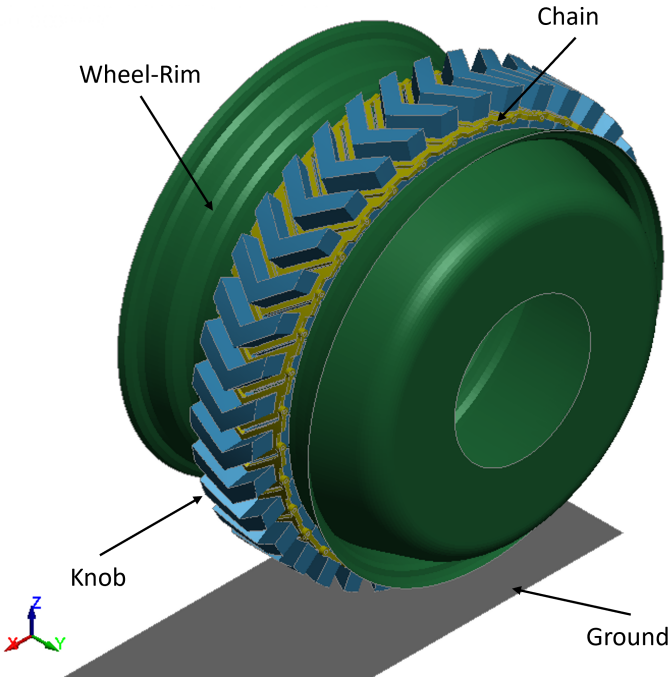

Figure 10. Graphic illustration of simulated configuration with the indication of different parts involved.

Table 3. Modeling characteristics of bodies involved in the analysis.

Body	Element	Formulation	Material Model
Wheel rim	Shell	Deformable	MAT015 Johnson-Cook
Chain (Belt)	Solid	Deformable	MAT015 Johnson-Cook
Knobs	Solid	Deformable	MAT077 Ogden Rubber
Ground	Shell	Rigid Body	MAT 020 Rigid

Interactions between bodies are modeled employing different types of contact formulations available in the simulation code. Contacts used are summarized in the contact matrix reported in Table 4.

Table 4. Contact Matrix.

	Wheel Rim	Chain (Belt)	Knobs	Ground
Wheel-Rim	-	-	Tied	-
Chain (Belt)	-	-	Tied	-
Knobs	Tied	Tied	Surf2Surf	Surf2Surf
Ground	-	-	Surf2Surf	-

The loading of the wheel was performed by displacing the rigid ground against the wheel until the desired force was reached, as reported in Table 1. A reversed motion was set up: the wheel assembly can only rotate about its axis, while the ground translates rigidly; the composition of motions determines pure rolling. Initial conditions are applied in terms of the velocity of the ground and wheel. The simulated translational velocity was set at 100 km/h, equivalent to about 28 m/s; the angular velocity applied to the wheel was 113 rad/s (associated with a rolling radius of 248 mm). To obtain the desired system kinematic, proper boundary conditions were applied to each body, as specified in Table 5.

Table 5. Indication of boundary condition system employed.

Body	Constrained DOF	Initial Conditions	Prescribed Motion
Wheel assembly: Rim + Chain + Knobs	Z, Y	Angular velocity about the rotation axis (parallel to Y axis)	-
Ground	Y	Y translational velocity	Z translation

Results of the simulation prove that, in the rolling phenomena, more than three knobs perform contact simultaneously, distributing the load properly (Figures 11 and 12). Contacting knobs deformation is such that a non-zero distance between the rim and the ground is ensured. A proper transition between knobs is attained in order to maintain a smooth rolling.

In Figure 13 is reported the interaction force between knobs and ground; an increase in load can be noticed at the beginning of the analysis due to the loading phase, wherein the transient is rapidly extinguished and a steady state rolling is reached. Slight load fluctuation can be appreciated due to alternating phases of loading and unloading of knobs. Figure 14 shows the normalized deformation of the knob during system rolling; knob experiences a maximum height reduction of about 25 % and its compression–release phase spans about 50°.

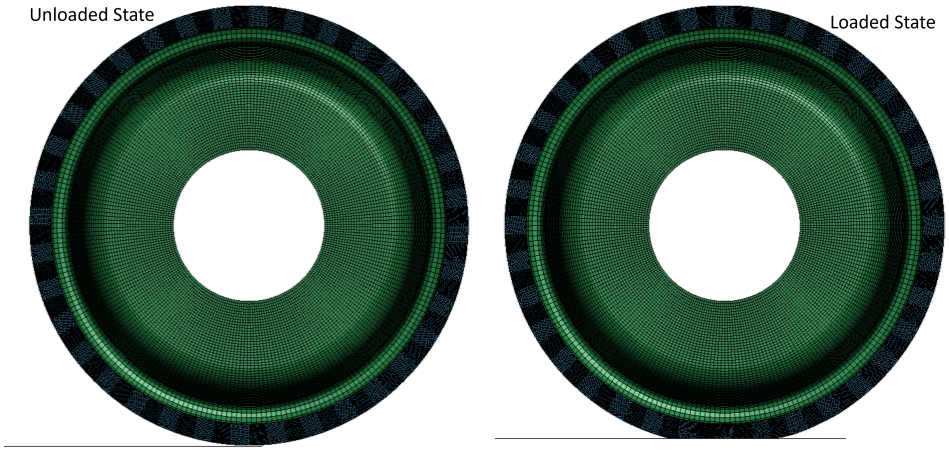

Figure 11. Post-process graphic illustration of the system in loaded and unloaded condition.

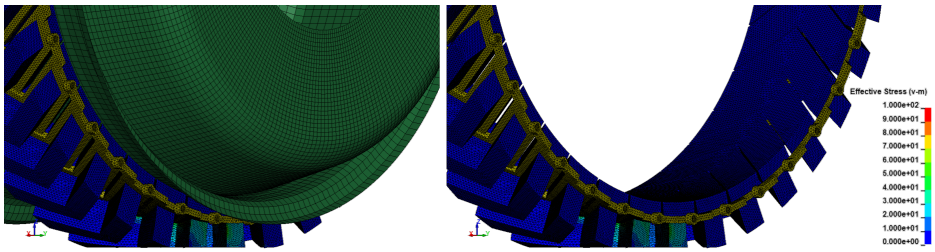

Figure 12. Detail of contacting knobs showing the fringe plot of the Von Mises equivalent stress (only active on knobs elements).

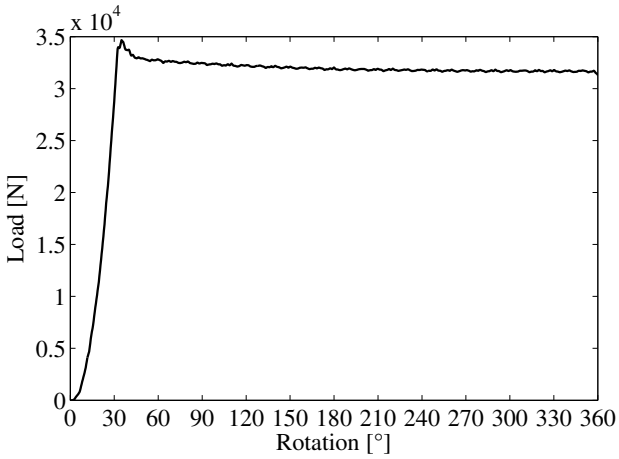

Figure 13. Interaction force between knobs and ground bodies.

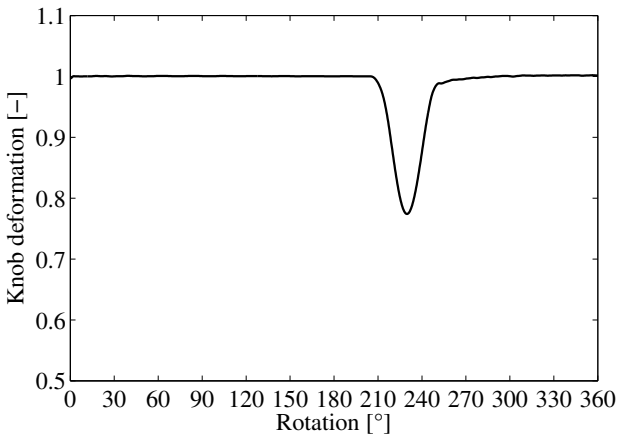

Figure 14. Knob deformation profile.

4. Prototyping

Following the preliminary design and analyses, a technological demonstrator was manufactured to verify with greater confidence the feasibility and functionality of the proposed system. Most effective strategies for rapid prototyping are based on additive manufacturing techniques. The potentials of this recently developed approach are manifold: the flexibility in terms of employable materials (metals, polymers, ceramics), flexibility in terms of achievable geometry, and the rapidity of the process [18–20]. The Hero-Belt prototype was manufactured applying a scale of 0.8:1; all major components were produced. Some geometrical simplifications were operated to ease the most critical manufacturing processes. Each element was produced using additive manufacturing techniques. The wheel rim and chain were manufactured using PLA material, employing a 3D printer based on the FFF (Fused Filament Fabrication) process, whose characteristics are reported in Table 6. A 1.75 mm Anycubic commercial filament was used to feed the printer extrusion.

Table 6. Overall characteristics referred to the 3D printer used for chain links and rim manufacturing.

Process Technology	Build Volume [mm]	Nozzle Temp.	Bed Temp.	Nozzle Size	Extruder Type
FFF	400 × 400 × 450	260°	90°	0.4 mm	Bowden

Since the most suitable materials to act as interface between wheel and road are elastomeric, knobs were manufactured using TPU (Thermoplastic Polyurethane) material. The scientific and industrial interest for this class of 3D printed materials has been growing in recent years [21,22]. The good trade-off in terms of strength, ability to withstand large deformations, and wear resistance, make this material appropriate for extreme applications. FFF techniques were employed to manufacture knobs, and the characteristics of the 3D printer used for this purpose are reported in Table 7. Geeetech commercial filament was used to feed the printer extrusion, having a hardness of 95 ShoreA and a diameter of 1.75 mm.

Table 7. Overall characteristics referred to the 3D printer used for knobs manufacturing.

Process Technology	Build Volume [mm]	Nozzle Temp.	Bed Temp.	Nozzle Size	Extruder Type
FFF	200 × 200 × 200	260°	100°	0.6 mm	Direct Drive

Printing process set-up was defined to obtain a good trade-off between printing quality and process duration, Table 8. The wheel rim was divided into three portions, manufactured in different print batches, and sequentially assembled. Some print previews provided by the slicing software are reported in Figures 15 and 16. Some examples of the obtained components are reported in Figures 17 and 18. After a few post-processing operations, all components were assembled to compose the Hero-Belt prototype, as shown in Figures 19 and 20.

Table 8. Overall printing process parameters.

Item	Filament	Nozzle Temp.	Bed Temp.	Layer Thickness	Avg. Print Speed
Chain link	PLA	206°	62°	0.15 mm	20 mm/s
Rim	PLA	206°	62°	0.15 mm	20 mm/s
Knob	TPU	245°	50°	0.20 mm	20 mm/s

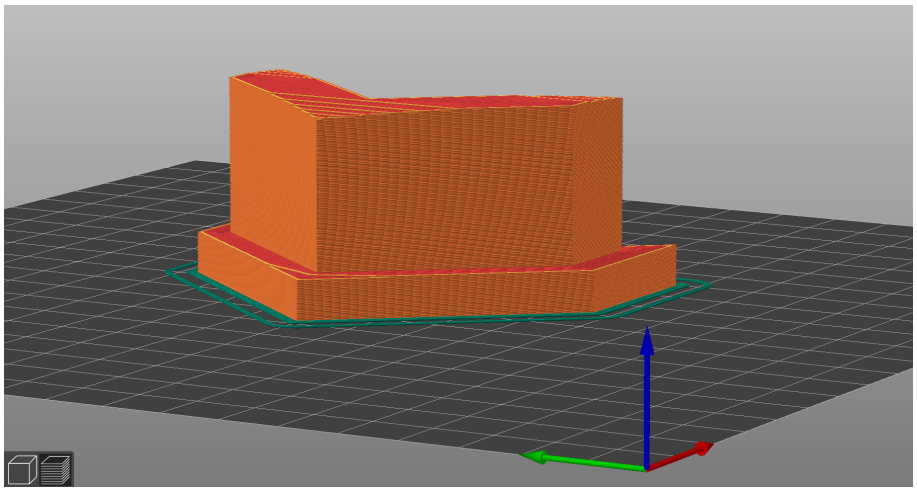

Figure 15. Print preview of knob slicing.

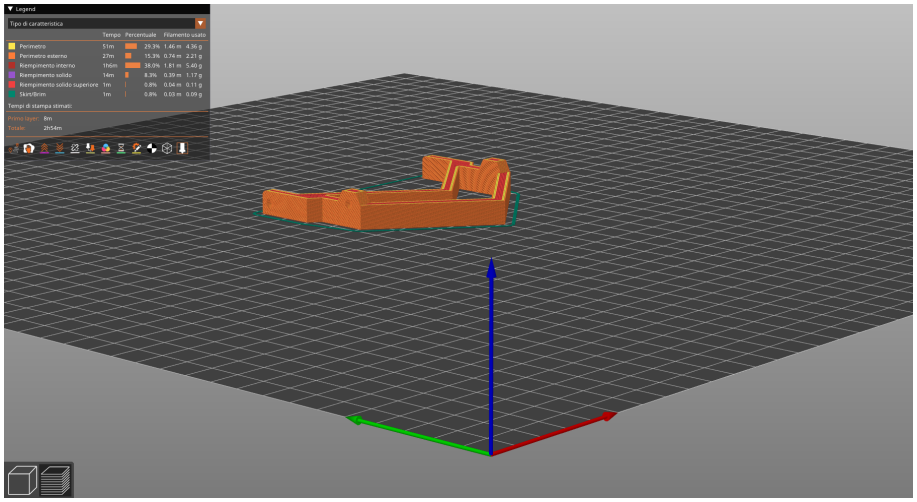

Figure 16. Print preview of chain link slicing.

Figure 17. Picture of knob after manufacturing process.

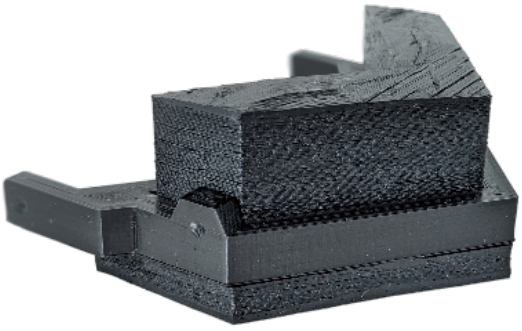

Figure 18. Picture of the manufactured sub-assembly: knob + chain link.

Figure 19. Hero-Belt chain (stand-alone).

Figure 20. Picture of complete Hero-Belt assembly prototype.

5. Conclusions and Way Ahead

A novel Run-Flat system for light/mid-weight vehicles was developed, and a concept design was released. Structural analyses were performed using numerical simulations on system assembly to verify structural resistance compliance and overall system operation. A simplified prototype was manufactured employing state-of-the-art prototyping

techniques. The activity proved the feasibility of the proposed solution and its potential, showing features that could make Hero-Belt a step forward in Run-Flat technology, as indicated by its following advantages:

- Enable the employment of Run-Flat technology for heavy-duty vehicles, associated to critical operating conditions.
- Modularity: possibility to employ the system independently from the tire or rim type.
- Potentially mitigate overheating phenomena of typical Run-Flat system.
- Mountable: easy to assemble and disassemble the Run-Flat system.

Additional activities to improve technology readiness can be the addition of thermal analysis of rolling knobs, to quantify the eventual enhancement of thermal dissipation. It is recognized that viscosity, strain rate, and temperature strongly influence this class of elastomeric materials, especially in applications associated to cyclic loading at medium/high frequency [23]. Different material models have been proposed and implemented in Ls-dyna keywords to account for the cited influencing parameters [24,25]. In spite of that, none of the ready-to-use models describe the heat generation due to viscous dissipation, for which a user-defined model approach is needed [26]. In addition to further numerical investigation, the development of test campaigns in operational conditions could provide more detailed information regarding system resistance, wear, and thermal performances.

Author Contributions: Conceptualization, N.B.; methodology, G.I. and G.T.; software, A.C.; validation, G.T., L.E. and A.C.; formal analysis, G.I.; writing—original draft preparation, A.C.; writing—review and editing, G.T. and N.B. All authors have read and agreed to the published version of the manuscript.

Funding: This study was carried out within the MOST – Sustainable Mobility Center and received funding from the European Union Next-GenerationEU (Piano Nazionale di Ripresa e Resilienza (PNRR)—Missione 4 Componente 2, Investimento 1.4—D.D. 1033 17/06/2022, CN00000023). This manuscript reflects only the authors' views and opinions, neither the European Union nor the European Commission can be considered responsible for them.

Institutional Review Board Statement: Not applicable.

Informed Consent Statement: Not applicable.

Data Availability Statement: Data are contained within the article.

Conflicts of Interest: The authors declare no conflicts of interest. The funders had no role in the design of the study; in the collection, analyses, or interpretation of data; in the writing of the manuscript; or in the decision to publish the results.

References

1. Cho, J.R.; Lee, J.H.; Jeong, K.M.; Kim, K.W. Optimum design of run-flat tire insert rubber by genetic algorithm. *Finite Elem. Anal. Des.* **2012**, *52*, 60–70. [CrossRef]
2. Haq, M.T.; Zlatkovic, M.; Ksaibati, K. Assessment of tire failure related crashes and injury severity on a mountainous freeway: Bayesian binary logit approach. *Accid. Anal. Prev.* **2020**, *145*, 105693. [CrossRef] [PubMed]
3. Markow, E.G. Run-Flat tire Incorporating Tape-Wrapped Helical Coil Band. Patent EP0205356A2, 17 April 1986.
4. Kopsco, M.A.; Markow, E.G. Segmented-Band Banded Tire. Patent EP0115129A2, 30 November 1983.
5. Zang, L.; Cai, Y.; Wang, B.; Yin, R.; Lin, F.; Hang, P. Optimization design of heat dissipation structure of inserts supporting run-flat tire. *Proc. Inst. Mech. Eng. Part D J. Automob. Eng.* **2019**, *233*, 3746–3757. [CrossRef]
6. Liu, H.; Pan, Y.; Bian, H.; Wang, C. Optimize design of run-flat tires by simulation and experimental research. *Materials* **2021**, *14*, 474. [CrossRef] [PubMed]
7. Motrycz, G.; Stryjek, P.; Jackowski, J.; Wieczorek, M.; Ejsmont, J.; Ronowski, G.; Sobieszczyk, S. Research on operational characteristics of tyres with run flat insert. *J. KONES Powertrain Transp.* **2012**, *16*, 319–326. [CrossRef]
8. Testa, G.; Bonora, N.; Esposito, L.; Iannitti, G. Design of an Electromechanical Testing Machine for Elastomers' Fatigue Characterization. *Eng. Proc.* **2025**, *85*, 21. [CrossRef]

9. Available online: https://www.continental-pneumatici.it/b2c/car/continental-tire-technologies/runflat-tires/ (accessed on 1 July 2024).
10. Available online: https://tech-outdoors.com/misc/how-does-run-flat-tires-work.html (accessed on 1 June 2024).
11. Available online: http://www.opony-samochodowe.com/blog/tag/seal-inside (accessed on 1 July 2024).
12. Phromjan, J.; Suvanjumrat, C. A suitable constitutive model for solid tire analysis under quasi-static loads using finite element method. *Eng. J.* **2018**, *22*, 141–155. [CrossRef]
13. Jebur, Q.H.; Jweeg, M.J.; Al-Waily, M.; Ahmad, H.Y.; Resan, K.K. Hyperelastic models for the description and simulation of rubber subjected to large tensile loading. *Arch. Mater. Sci. Eng.* **2021**, *108*, 75–85. [CrossRef]
14. Ogden, R.W. Large deformation isotropic elasticity—On the correlation of theory and experiment for incompressible rubberlike solids. *Proc. R. Soc. Lond. A Math. Phys. Sci.* **1972**, *326*, 565–584. [CrossRef]
15. Benam, A.A. Comparative modelling results between a separable and a non-separable form of principal stretches–based strain energy functions for a variety of isotropic incompressible soft solids: Ogden model compared with a parent model. *Mech. Soft Mater.* **2023**, *5*, 2. [CrossRef]
16. Huang, L.; Yang, X.; Gao, J. Pseudo-elastic analysis with permanent set in carbon-filled rubber. *Adv. Polym. Technol.* **2019**, *2019*, 2369329. [CrossRef]
17. Fu, X.; Wang, Z.; Ma, L. Ability of constitutive models to characterize the temperature dependence of rubber hyperelasticity and to predict the stress-strain behavior of filled rubber under different defor mation states. *Polymers* **2021**, *13*, 369. [CrossRef] [PubMed]
18. Bertocco, A.; Iannitti, G.; Caraviello, A.; Esposito, L. Lattice structures in stainless steel 17-4PH manufactured via selective laser melting (SLM) process: Dimensional accuracy, satellites formation, compressive response and printing parameters optimization. *Int. J. Adv. Manuf. Technol.* **2022**, *120*, 4935–4949. [CrossRef]
19. Callanan, J.G.; Martinez, D.T.; Ricci, S.; Derby, B.K.; Hollis, K.J.; Fensin, S.J.; Jones, D.R. Spall strength of additively repaired 304L stainless steel. *J. Appl. Phys.* **2023**, *134*, 245102. [CrossRef]
20. Ricci, S.; Zucca, G.; Iannitti, G.; Ruggiero, A.; Sgambetterra, M.; Rizzi, G.; Bonora, N.; Testa, G. Characterization of Asymmetric and Anisotropic Plastic Flow of L-PBF AlSi10Mg. *Exp. Mech.* **2023**, *63*, 1409–1425. [CrossRef]
21. Kechagias, J.D.; Vidakis, N.; Petousis, M. Parameter effects and process modeling of FFF-TPU mechanical response. *Mater. Manuf. Process.* **2021**, *38*, 341–351. [CrossRef]
22. Ricci, S.; Pagano, A.; Ceccacci, A.; Iannitti, G.; Bonora, N. An Investigation of the Monotonic and Cyclic Behavior of Additively Manufactured TPU. *Eng. Proc.* **2025**, *85*, 18. [CrossRef]
23. Schieppati, J.; Schrittesser, B.; Pinter, G. Heat build-up of rubbers during cyclic loading. In Proceedings of the European Conference on Constitutive Models for Rubber—ECCMR, Nantes, France, 25–27 June 2019.
24. Krishnan, G.; Savic, V.; Cordeiro, B.; Biswas, S. Evaluation of Viscoelastic Material Models in LS-DYNA based on Stress Relaxation Data. In Proceedings of the International LS-DYNA Conference, Plymouth, MI, USA, 22–23 October 2024.
25. Kolling, S.; Bois, P.A.D.; Benson, D.J. A Simplified Rubber Model with Damage. In Proceedings of the International LS-DYNA Conference, Bamberg, Germany, 20–21 October 2005.
26. Xu, H.; Zhou, J.; Cao, X.; Miao, C. A viscoelastic-viscoplastic thermo-mechanical model for polymers under hypervelocity impact. *Int. J. Mech. Sci.* **2024**, *272*, 109205. [CrossRef]